Kufa Journal of Engineering
Vol. 17, No. 2, April 2026, P.P. 528-541
Article history: Received 28 June 2025, last revised 13 August 2025, accepted 13 August 2025

AN EXPERIMENTAL STUDY OF THE EFFECT NANO-SILICA MADE FROM NATURAL SAND ON THE CORROSION RATE OF LOW CARBON STEEL

Samer Noaman Shattab[1] and Kadhim F. Alsultani[2]

[1] Chemical Engineering Department, College of Engineering, University of Babylon, Iraq, Email:eng435.sammer.noaman@student.uobabylon.edu.iq.

[2] Chemical Engineering Department, College of Engineering, University of Babylon, Iraq, Email:finteelalsultani@gmail.com.

https://doi.org/10.30572/2018/KJE/170232

ABSTRACT

This study demonstrated the effectiveness of laboratory-prepared nano-silica derived from Iraqi natural sand using sol-gel technology in providing effective corrosion protection. The inhibitor was evaluated on low-carbon steel surfaces using dynamic polarization, Tafel plots, polarization curves, and weight loss. Concentrations of 400-1000 ppm and temperatures of 25-55°C were used for the study. The results indicated that the synthesized inhibitor was highly effective in reducing corrosion by forming a thin film on the surface of A106 Grade B steel. while the weight loss ranged from 95.8-76.4% in 1M-HCl medium. Characterization methods such as FTIR, SEM, XRD, and AFM were used to study the preparation process and evolution of the protective layer. The results indicated the stability of the protective activity of the inhibitor. The performance was described as economical, sustainable, scalable, highly efficient, and low toxicity.

KEYWORDS

Polarization; Electrical Impedance; Iraqi sand; Nano-silica; Sol-gel; Green Inhibitors.

1. INTRODUCTION

Corrosion of carbon steel is a common problem in industrial applications (Al-Amiery et al., 2023). Corrosion caused by environmental exposure and operating conditions significantly deteriorates metal structures, both internal and external surfaces (Kadhum & Mohammed, 2024). Carbon steel is classified into three grades: low, medium, and high, based on its carbon content. Low-carbon steel is more economical and easier to use (Tawfik et al., 2019). This is due to its unique properties, including a yield strength range of 250 to 1380 MPa, mechanical strength, formability, weldability, and corrosion resistance thanks to the oxide layer on the metal surface (Yousif & Ataiwi, 2018). Carbon steel often encounters various corrosive agents, particularly in the petroleum sector, especially in acidic conditions (Jaddoa et al., 2025). Crude oil consists of organic and sulfur compounds, in addition to chloride salts (NaCl, KCl, $MgCl_2$ and $CaCl_2$) dissolved in the reservoir water accompanying the oil from the well (Shatab et al., 2023). During crude oil distillation processes in refining units. Consequently, these media cause corrosion of metal components in pipes and refining equipment, especially in the crude oil preheating zone in heat exchangers and in the air exchangers for petroleum products above the distillation tower, as well as in the pipes that transport the heated oil from the furnace zone to the primary crude oil distillation tower. Many environmental conditions affect the corrosion of metal materials in the petroleum industry, including pH, temperature, salinity, and humidity levels (Mohammed, 2023). All these factors interact and significantly impact the lifespan of metal materials. To mitigate these effects and maintain the structural integrity of the metal, a variety of preventive methods are used, including cathodic protection, barrier coatings, and environmentally friendly organic and inorganic chemical corrosion inhibitors. Corrosion inhibitors are considered one of the most effective means of protecting steel equipment and pipes from corrosion (AlGhali et al., 2025). These inhibitors work by adsorption to the metal surface, blocking many active corrosion sites. However, synthetic inhibitors often pose risks to human health, industrial safety, and the environment, making their use dangerous. Furthermore, they are often expensive due to their industrial origins (Hammouti et al., 2012). In contrast, natural corrosion inhibitors are environmentally friendly, safe, sustainable, easy to use, effective, and low-cost. They also provide effective protection against metal degradation. Previous studies on sustainable green corrosion inhibitors have shown their effectiveness under hostile conditions by creating a thin protective layer on metal surfaces, thereby protecting the underlying oxide layers. Bashir Abdul Hassan et al. used a natural silicate-based inhibitor in a 1 M sulfuric acid solution to reduce the corrosion of petroleum tank alloys (ASTM A285 Grade C), achieving an inhibition efficiency of 91.6% (Abdulhussein et al., 2023). Hajer et al. used

turmeric-derived green inhibitors to protect low-carbon steel (ASTM A283) in a 3.5% sodium chloride solution, achieving an efficiency of 97.52% (Jaddoa et al., 2025). Pramodita et al. improved the corrosion resistance of mild steel by incorporating rice husk-derived silicon dioxide (SiO_2) nanoparticles, facilitating the development of a stable inhibitory layer on the metal surface (Saputra et al., 2025). Taheri et al. formulated an environmentally friendly inhibitor consisting of amino acids and zinc oxide (ZnO) nanoparticles, demonstrating a maximum inhibition efficiency of 87.62% in 1 M hydrochloric acid at 30 °C when applied to carbon steel (Taheri et al., 2017). Alvarez et al. al. developed green inhibitors specifically for mild steel applications using gum Arabic and silver nanoparticles, achieving inhibition efficiencies of 93% in hydrochloric acid and 91% in sulfuric acid (H_2SO_4) environments (Alvarez et al., 2018). Kamburova et al. investigated hibiscus leaf extract as an environmentally friendly inhibitor for mild steel in 0.1 M hydrochloric acid and observed the development of a protective layer that significantly improved corrosion resistance (Kamburova et al., 2021). Asaad and Mohammed investigated the functionality of green inhibitors derived from plant and fruit wastes in the oil and gas sector, confirming their effectiveness in mitigating corrosion in various crude oil processing systems (Asaad et al., 2018). The sol-gel method is widely used in the manufacture of metal oxide nanoparticles due to its ability to form homogeneous nanostructures in good quantities. This research aims to synthesize and evaluate a silica (SiO_2) nanoparticle extract derived from natural sands obtained from the soil of Najaf, Iraq, using the sol-gel method, as environmentally friendly corrosion inhibitors. This method was applied to low-carbon steel (ASTM A106 Grade B) used in Iraqi oil refineries as the target metal in the current work. Dynamic polarization and weight loss experiments were performed in 1 M HCl solution to evaluate the inhibitory activity and protective properties, along with other characterization studies, according to sustainable corrosion prevention methodologies.

2. EXPERMENTAL PART

2.1. FEEDSTOCK

2.1.1. RAW MATERIAL

Natural sand from Najaf, Iraq, was used to produce silica nanoparticles, which were subsequently used as an environmentally friendly corrosion inhibitor in this study. A sample of untreated sand was collected for chemical analysis using XRF technology. The percentages of natural sand components (%) were as shown in Table 1.

Table 1. Chemical composition of raw sand based on XRF analysis.

Component	SiO_2	Al_2O_3	Fe_2O_3	Na_2O_3	LOI	Other
Wt%	95.7	0.4	1.41	0.05	1.25	1.19

2.1.2. SPECIMENS

The present study used metal parts made of low-carbon steel pipes (ASTM A106 Grade B, Chemtech Alloys, Ukraine, SCH 40 NO 210091). The chemical composition test was performed using a Spectro max apparatus at 25°C, as shown in Table 2. All metal components were pre-treated, including initial polishing using an MP-2B polishing machine under a stream of clean water and sandpaper of grades 250, 400, 600, 800, 1000, 1200, and 1400. The samples were rinsed with deionized water, cleaned with acetone, and dried. A polishing gel was used for secondary polishing to create a mirror-like surface. The present work used 1 M hydrochloric acid as the corrosion medium. Fig. 1 illustrate the metal samples before and after cutting and processing with the used apparatus.

Table 2. Analysis of the chemical composition of A106 Grade B carbon steel by Spectro Max at 25°C (XRF).

Element	Fe	P	C	Mn	Cr	S	Cu	Ni	ether
Wt %	Balance	0.0172	0.211	0.40	0.0377	0.0104	0.169	0.0523	0.1024
Normal	Balance	0.035	0.230	0.129	0.14	0.035	0.24	0.04	0.151

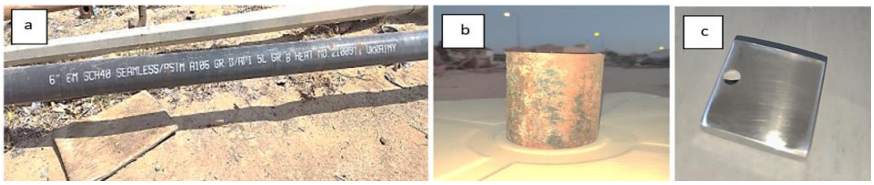

Fig.1. a: illustrate the tubes in situ, b: tube model, c: weight loss samples.

2.1.3. SILICA PREPARATION

The present work utilized a top-down approach to synthesize silica nanoparticles Fig. 2. 60 grams of high-purity sand was used. The sand was continuously rinsed with distilled water while stirring to remove dust and impurities and then screened in two stages using a regular household sieve and a fine sieve (College of Materials Engineering, University of Babylon). The sand was subsequently dried for 5 hours at 120°C. After washing for 20 minutes with 0.1 M dilute hydrochloric acid using a magnetic stirrer, suspended solid impurities were removed. After washing with deionized water, drying was carried out at 110°C for 5 hours. The sand was then processed in a home grinder to reduce particle size. (60) grams of the resulting sand were thoroughly mixed with (80) grams of caustic soda, then heated to 400°C for 35 minutes until water bubbles appeared, indicating the completion of the reaction to produce hydrated sodium silicate Eq.1 (Shattab & Alsultani, 2025). The product was then cooled, and sodium silicate was dissolved in 600 mL of deionized water with continuous stirring for 20 min to ensure complete dissolution. The product was filtered and collected in a 1000 mL vessel. Then, concentrated sulfuric acid was gradually added until a white silica gel Eq.2 was formed (Shnaihej et al., 2019). The pH value was measured and determined to be 1.2 (Mahmood et al., 2022).

$$Sand(natural) + 2NaOH \rightarrow Na_2SiO_3 + H_2O \quad (1)$$

$$Na_2SiO_3 + H_2SO_4 \rightarrow 3SiO_2(gel) + Na_2SO_4 + H_2O \quad (2)$$

The resulting silica gel was repeatedly washed with deionized water for purification, and then dried at 110°C for 24 hours in the laboratory (College of Chemical Engineering, University of Babylon, Iraq) to yield a pure, white, highly porous silica powder. Finally, 15 grams of the produced silica powder was ground for 12 hours using an NQM-0.4 model planetary ball mill at the Nanotechnology and Advanced Materials Research Center (Baghdad, Iraq), University of Technology, to obtain pure silica with a size of 95.5 nm, synthesized using the sol-gel technique from natural sand.

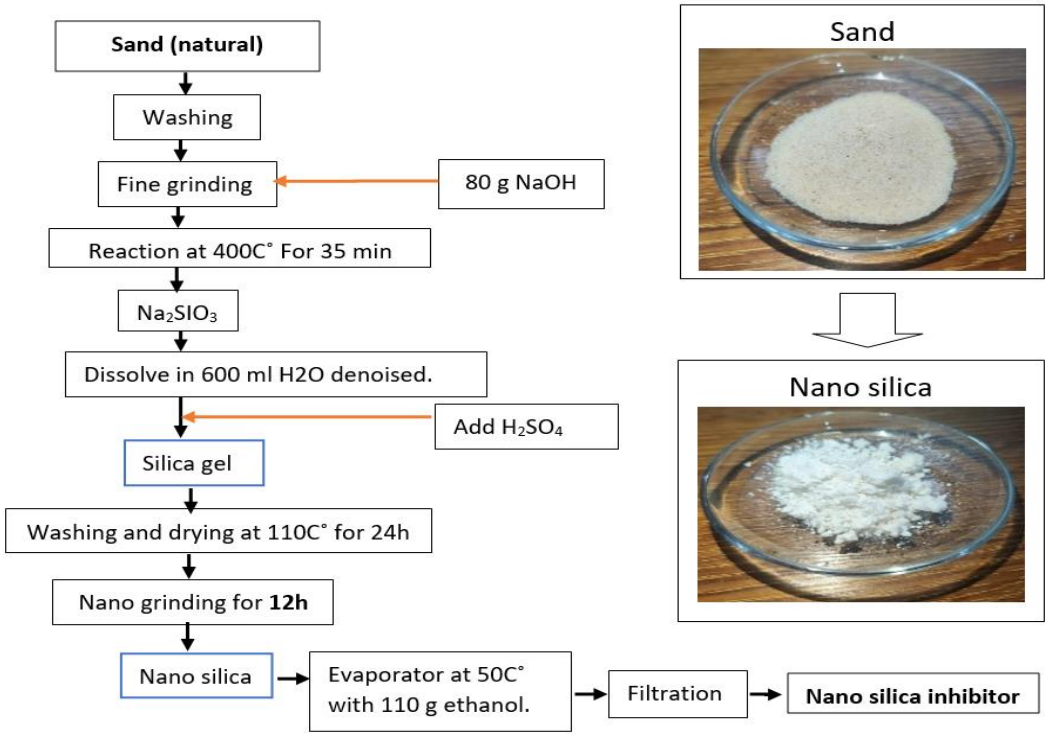

Fig.2. Schematic representation for preparing silica extract from natural sand.

2.1.4. NANO SILICA INHIBITOR SYNTHESIS

Five grams of the previously synthesized nano silica was measured and dissolved in a 250-ml beaker containing 100 ml of methanol as a solvent, under continuous stirring, and gradually heated to a temperature range of 25–55°C for 50 min using a reflux condenser. The solution was filtered for four hours to obtain a final quantity of 50 ml of silica extract.

2.2. EXPERIMENTAL TEQNIQUE PART

2.2.1. POLARARIZATION & IMPEDANCE CURRENT

To conduct the polarization experiments, in addition to Tafel, a 250 ml electrochemical cell was used with three electrodes: a potassium chloride-saturated calomel (SCE), a graphite electrode, and a target sample electrode (A 106°B) with a geometric area of 1 cm^2. After 30

minutes of constant voltage, the Ecorr polarization curves were independently obtained. Dynamic current-voltage curves were generated by shifting the electrode potential at 0.5 mV/s. Data analysis was performed using CORRTEST (version 6.3). Using the algorithm, the optimal values for βa, βc, Ecorr, and Ecorr were statistically found. The presence and absence of a corrosion inhibitor were tested at 25, 35, 45, and 55 °C. A water bath (Turkish-made BS-21) controlled the temperatures. Eight experiments were conducted to measure corrosion rates under various conditions using the polarization method, polarization curves (four experiments without inhibitors and four experiments with inhibitors). The experiments were conducted in the laboratories of the Nano and Advanced Materials Research Center in Baghdad, Iraq. The samples underwent a 15-minute polarization curve test.

2.2.2. WEIGHT LOSSES

Weight loss techniques were used to compare corrosion rates in acidic media with and without 1 M hydrochloric acid. Sample weights before and after corrosion were calculated using a sensitive four-level balance (0.0001). A 250 ml experimental vessel was used. Weight loss studies were conducted in the corrosion laboratories of the University of Babylon, Iraq, and lasted for 1 hour. The studies were conducted at temperatures of 25, 35, 45, and 55 °C with and without a silicate inhibitor (PPM) (400, 600, 800, and 1000). Eight weight loss studies were conducted. Samples were subjected to a 60-minute weight loss test.

3. RESULTS AND DISCUSION

3.1. CHARACTERIZATION ANALYSES

Fig.3 shows the X-ray diffraction (XRD) pattern of silicon oxide nanoparticles synthesized from natural Iraqi sand. Their properties are mainly determined by the crystal structure and chemical composition of the sand. After repeatedly washing the sand with deionized water and dilute (1M-HCl) solution, excellent results were obtained for the preparation of pure silica by the sol-gel method. Scherrer equation calculations indicated the presence of nanoscale, confirming the validity of the results Eq.3 (Vorokh, 2018) .

$$D = K\lambda / (\beta\cos\theta) \quad (3)$$

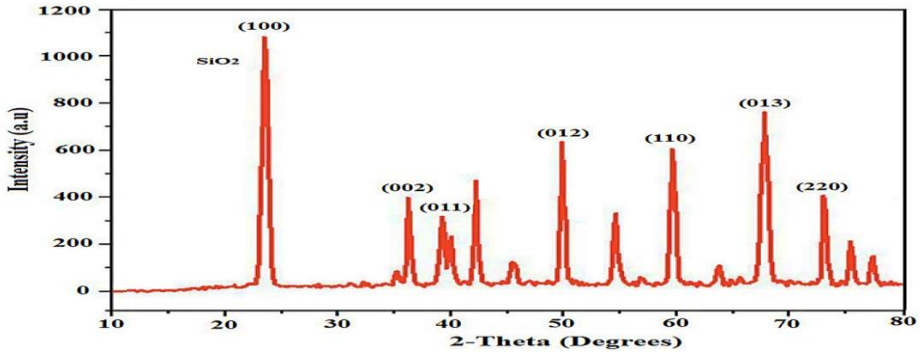

Fig. 3. XRD pattern of silica nanoparticles

Fig.4 illustrates the Fourier transform infrared (FTIR) spectroscopy methodology used to identify the chemical bonds present in the silica molecule as functional groups. Fig. 4 shows the FTIR spectra of SiO_2 NPs synthesized from Iraqi sand. The characteristic SiO_2 bands at 1047 cm-1 and 795 cm-1 correspond to the Si–O–Si symmetric band and Si–OH stretching band, respectively. The peaks indicate the stretching vibrations of the asymmetric groups within the Si–O–Si bond and the silanol, providing evidence of the underlying silicate network structure for interactions at the metal surface. At wavelengths of 1631 and 2818 nm, the OH and H–O–H stretching vibrations are seen, respectively. These bands indicate the presence of surface hydroxyl groups and bending vibrations of water molecules adsorbed on the silica surface, which increases corrosion inhibition on the metal surface. Moreover, the peaks at 3391–2818 cm-1 and 750–650 cm-1 arise from C–H stretching and N–H vibrations, respectively. The band in the absorption region at 438 cm-1 is associated with the asymmetric stretching vibrations of the Si–O group (Wang et al., 2014).

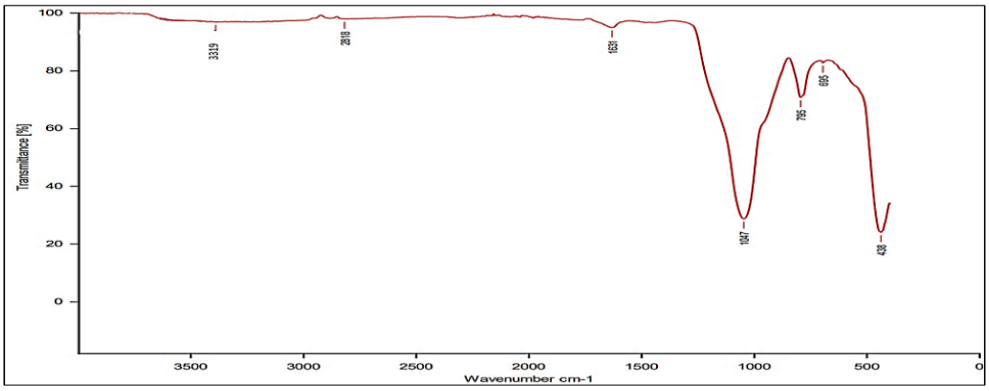

Fig. 4. FTIR spectrum for silica nanoparticles.

Fig. 5(a-b) Scanning electron microscope (SEM) results of the metal and silicon dioxide (SiO_2) nanoparticle samples. Fig. 5(a) shows the metal surface after immersion in a corrosive medium of 1 M hydrochloric acid without the addition of a silicate inhibitor. Fig.5(b) shows a thin, evenly distributed silicate layer on the metal surface, which will act as a barrier to corrosion. To validate the results, Fig. 5(b) was examined at a concentration of 400 ppm, where the nano-silica inhibitor achieved an optimal protection efficiency (EI%) of 97.7%.

Fig.6 (a-c) Atomic force microscope (AFM) images show that the nano-silica inhibitor extracted from Iraqi Najaf sand can preserve the steel surface, especially at 25°C in a 1M-HCl medium with a 400-ppm silica additive concentration, where the silicate inhibitor achieved the highest efficiency. The dispersion ratios of the nanoparticle aggregates on the low-carbon steel sample are shown in Fig. 6a. A thin, evenly distributed layer form on the sample surface after adding the 400-ppm concentration, with three-dimensional atomic resolution in Figs. 6b, c. The surface histograms of the target low-carbon steel surfaces indicated a roughness of 96.76 nm.

AFM examination revealed how the silicate particles form a thin layer on the target metal surface to protect it from the corrosive medium. This is due to the even distribution of inhibitor molecules on the low-carbon steel surfaces and the cohesion of the protective layer.

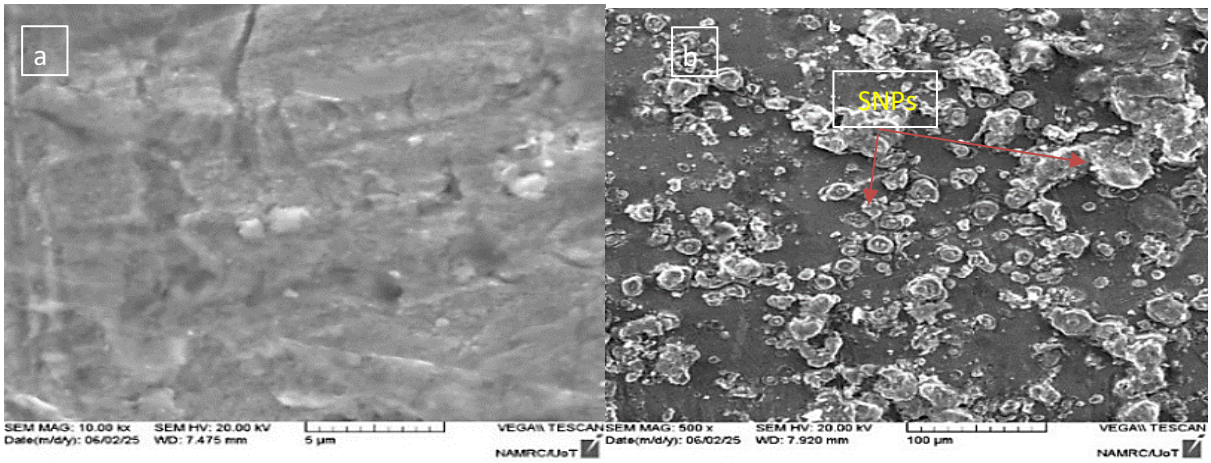

Fig. 5. SEM images: (a) metal surface corrosive without inhibitor, (b) thin layer of SiO_2

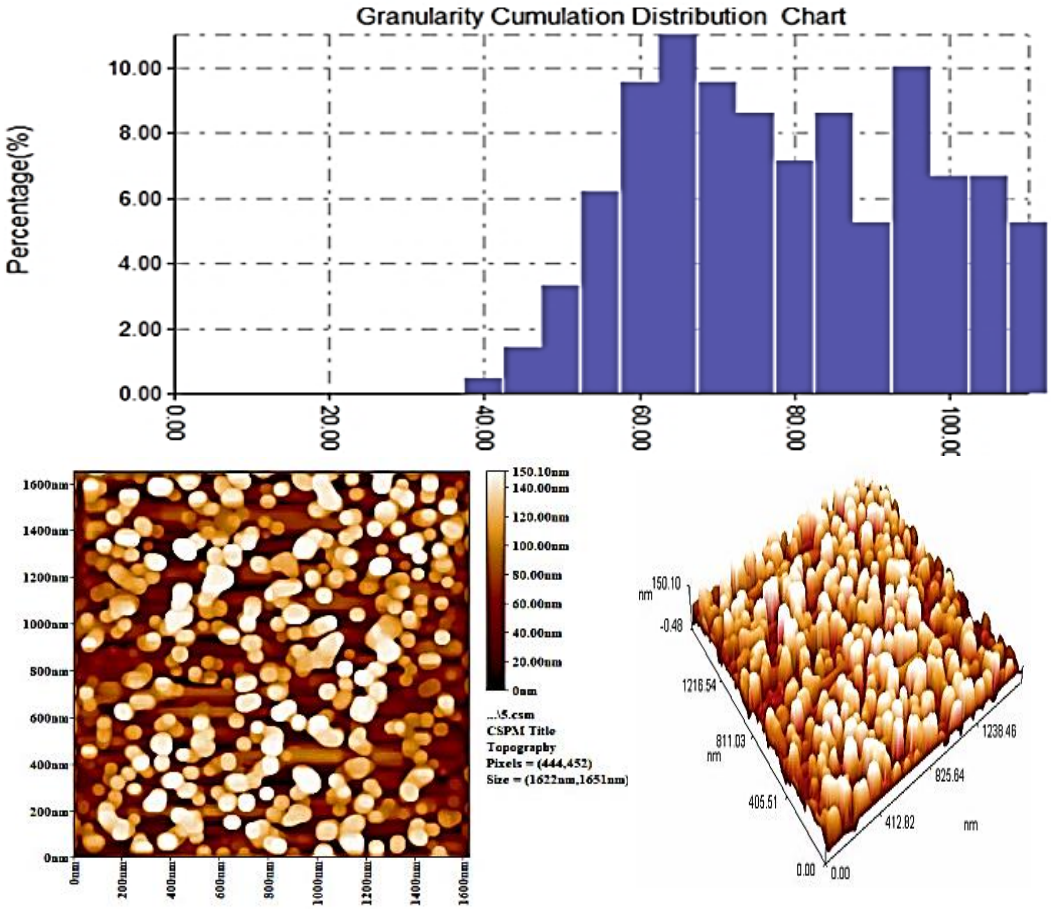

Fig. 6. a: Particle size distribution of Silica NPs, (b, c) 3D pictures.

3.2. EVALUATION TEQNIQUES

3.2.1. DYNAMIC POLARIZATION

Table 3 presents the polarization corrosion results of carbon steel (ASTM A106 grade B) using

different concentrations of silica nanoparticles (SiO_2) as an environmentally friendly corrosion inhibitor. The analysis was conducted using nanoparticle additives at concentrations of 400, 600, 800, and 1000 ppm at temperatures ranging from 25, 35, 45, and 55°C. The relationship between anode voltage and current density was studied. The corrosion process was also studied in 1M-HCl, Fig. 7a: Tafel plots for blank, Fig. 7b: Tafel plots with concentration of inhibitor silica). The results in Table 1 show that the concentration of the added nanoparticle affects the corrosion rate and current density. The cathodic response decreased at lower current densities. The results indicate that the (SiO_2-NPs) inhibitor significantly reduces anodic corrosion, especially for 400 nanoparticles at 25°C. While at a concentration of 1000 at 55°C, the inhibitory efficiency dropped to 90.9%, the inhibitor maintained its high performance. The reduced efficiency was attributed to a somewhat heterogeneous accumulation of the inhibitor and variable adsorption of the inhibitor on the metal surface. Efficiency was exceptional at concentrations of 400, 600, and 800 at temperatures ranging from 25, 35, and 45°C, respectively. The inhibitor exhibited superior inhibitory activity, resulting in the formation of a thin protective layer on the target metal surface. The thin layer on carbon steel provided superior corrosion protection compared to the original sample without the nanoparticle inhibitor.

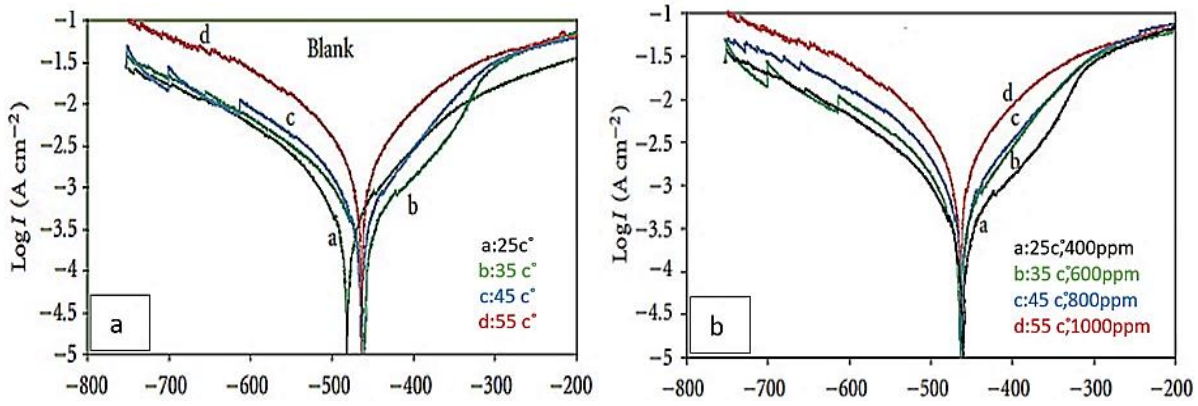

Fig. 7. (a) Tafel diagrams of blank experiments, (b) Tafel diagrams of track addition

Table 3. Electrochemical parameters and corrosion rate assessments using the dynamic polarization technique.

Run	Temperature (C°)	Concentration (ppm)	Open circuit potential (OCP) V	Ba (mv)	Bc (mv)	Corrosion carnet density (icoor) (Amps/cm2)	Corrosion potential (Ecoor) (v)	Corrosion rate (C.R) (mpy)	IE%
1	25	blank	-0.59136	156.79	-78.27	2.4264E-5	-0.76473	0.28454	-
2	35	blank	-0.45742	146.98	-87.54	2.11268E-5	-0.79897	0.30298	-
3	45	blank	-0.56490	17.45	-20.87	1.79864E-5	-0.90876	0.43421	-
4	55	blank	-0.54564	77.87	-87.99	1.39980E-5	-0.98897	0.56565	-
5	25	400	-0.39797	19.608	-19.42	5.4318E-7	-0.4114	0.0063722	97.7
6	35	600	-0.50898	24.794	-18.62	1.0972E-06	-0.51437	0.012872	95.5
7	45	800	-0.5263	26.924	-31.21	2.1967E-06	-0.55072	0.02577	90.9
8	55	1000	-0.43462	31.948	-25.25	3.0257E-06	-0.45549	0.035495	87.5

3.2.2. EVALUATION WEIGHT LOSS

The corrosion rate was evaluated using the weight loss method. The sample weights were accurately calculated and recorded before and after each experiment. A sensitive balance was used to calculate the weight difference between the two samples. Eqs.4, 5 show the corrosion rate and efficiency values for experiments (5-8) using nano silica inhibitors (400, 600, 800, and 1000 ppm), while for experiments (1-4) without the inhibitor, Table 4. At lower concentrations, especially 400, the inhibitor achieved the highest efficiency at 25 °C, with a corrosion rate of 0.0408 mA/h and an efficiency of 95.8%. At a concentration of 1000 ppm at 55 °C, the inhibitor achieved a corrosion rate of 5.6325 mpy and an efficiency of 76.4%. The inhibitory nanoparticles (95.6 nm) increased their surface area and contact with the metal surface, promoting homogeneous particle aggregation or uniform dispersion, and forming cohesive bonds on the metal surface. This formed an adsorbent layer that resisted corrosion, especially at low concentrations. Conversely, as the concentration increased, the corrosion efficiency decreased with increasing temperature. However, the inhibitor maintained good efficiency despite a significant increase in temperature of 10°C per temperature level. Consequently, the nanoparticle mobility improved with moderate increases in temperature, enhancing the effect of the inhibitor concentration. Inhibitors are typically resistant to metal surface attacks. On carbon steel, SiO_2 nanoparticle inhibitors-initiated adsorption. Concentration, corrosion duration, temperature, and corrosive medium significantly affect the inhibition effectiveness. Lower inhibitor levels improved inhibition performance. This study found that the produced SiO_2 nanoparticle inhibitor formed a thin protective adsorption layer on A106 Grade B carbon steel in 1 M hydrochloric acid solutions, preventing corrosion.

$$\text{Corrosion rate (CR)} = \frac{534*\text{W}}{\text{d}*\text{A}*t} \quad (4)$$

$$\text{IE} = \frac{CR\ blank - CR\ with\ inhibitor}{CR\ blank} * 100 \quad (5)$$

CR = mill per year (mpy), W = weight loss (g), d = specimen density (gm/cm^3), A = specimen surface area (in^2), and t = exposure period (Ivosevic et al. 2021).

Table 4. Results of using the weight loss technique to measure corrosion rates and efficiency with and without silicate inhibitor.

Run	Concentration (Ppm)	Temperature (C°)	Time (hr)	W1 (g)	W2 (g)	ΔW (g)	CR (mpy)	IE %
1	Blank	25	1	30.0001	29.9732	0.0269	0.9161	-
2	Blank	35	1	30.3216	29.9991	0.3225	10.9830	-
3	Blank	45	1	30.5432	29.9803	0.5629	19.1701	-
4	Blank	55	1	30.9999	28.3011	0.6988	23.9204	-
5	400	25	1	29.5839	29.5827	0.0012	0.0408	95.8
6	600	35	1	30.9964	30.9713	0.0251	0.8548	92.2
7	800	45	1	30.6135	30.5511	0.0624	2.1360	88.8
8	1000	55	1	30.1901	29.9999	0.1902	5.6325	76.4

Table 4 lists the results of experimental studies using the weight loss method under the influence of temperature and concentration variations on corrosion rate and efficiency values, with and without the addition of a silicate corrosion inhibitor to the 1 mol-HCl corrosion medium, using the target test sample (A106 Grade B). Most studies show that temperature increases the corrosion rate (CR) and reduces the IE%. The weight loss approach without the addition of a corrosion inhibitor demonstrated the effect of temperature on corrosion rate, with significantly increased corrosion values without the inhibitor. The effect of temperature on corrosion rate with the inhibitor was also observed, with values decreasing compared to those without the inhibitor, achieving effective inhibition. Efficiency values decreased with increasing temperature. However, the inhibition levels maintained by the inhibitor were within the range of (95.8 - 76.4), a very acceptable indicator of effectiveness Fig. (8a) , Fig. (8b) illustrates the effect of varying concentrations on corrosion rate and efficiency. The addition of inhibitor dosages resulted in reduced corrosion rates. Equation 6 calculates weight loss rates at a constant time (1 hour), a temperature (°C) of (25, 35, 45, 55) ± 1, and a sample area of (2.04) ± 0.001 square inches. Comparing the corrosion rates in Tables 3, 4, we find that the effect of temperature on corrosion rate is much greater when no inhibitor is used than when it is used. Both approaches may attribute the polarization and weight loss to the effectiveness of the inhibitor, which isolates the metal from the corrosive solution by forming a durable, protective layer.

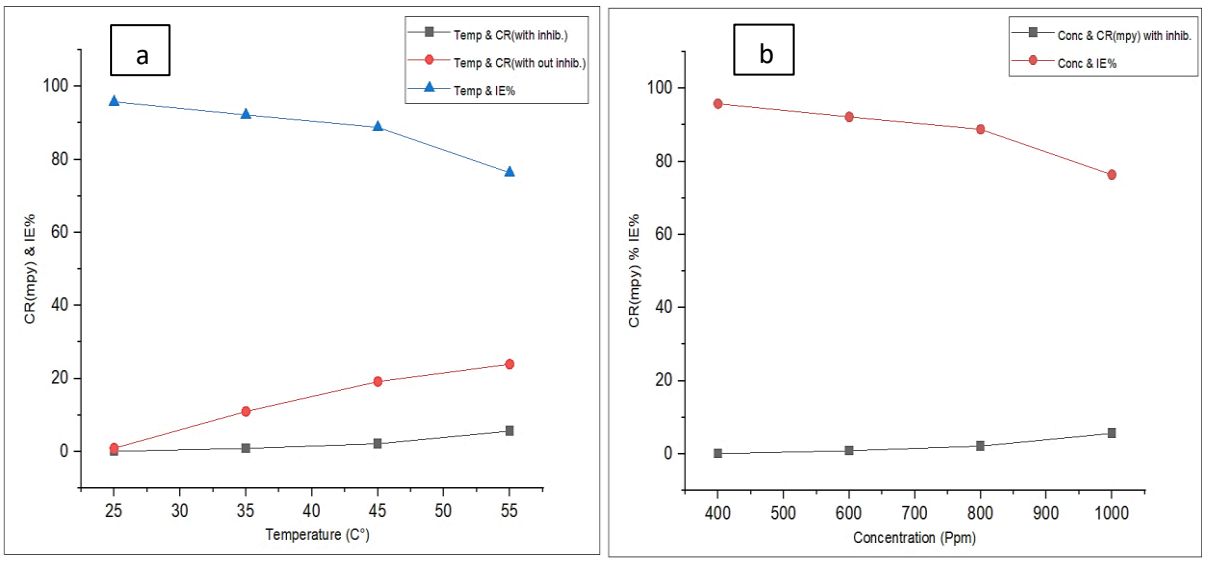

Fig. 8. Effect of weight loss method on corrosion rate A: temperature, B: concentration.

4. CONCLUSION

1. This study successfully extracted silica nanoparticles from natural sand using the sol-gel method in a laboratory setting and evaluated their effectiveness as a safe and environmentally

friendly corrosion inhibitor for ASTM A106 Class B steel pipes widely used in the crude oil refining sector.

2. Dynamic polarization and weight loss measurements showed that the nano-silica inhibitor, when applied at concentrations between 400 and 1000 ppm in a hydrochloric acid solution (1 mol-HCl), achieved high inhibition efficiencies ranging from 97.7% to 90.9% using the polarization technique, and 95.8% to 76.4% using the weight loss technique, over a temperature range of 25 to 55°C.

3. The overall results of the tests and evaluation experiments indicate an effective reduction in corrosion by blocking the anodic and cathodic reaction sites on the steel surface.

4. The nature of nano silica preparation is one of the biggest obstacles to nanoparticle production. Variables affecting nano size include humidity, ball size in the nano mill, mill rotation speed, and precise handling of the nanoparticles.

5. The current study encourages further research efforts into the use of nanostructures to improve their applications in corrosion control, and the use of nano silica at various concentrations and temperatures to demonstrate its ability to meet corrosion challenges and achieve sustainable protection.

5. REFRANCES

Abdulhussein, B. A., Ali, A. M., & Sukkar, K. A. (2023). Reducing corrosion attacks on carbon steel A285 grade C in petroleum storage tanks by forming a thin film of nano- SiO_2 from sand. Chemical Papers, 77(3), 1533–1543. https://doi.org/10.1007/s11696-022-02571-9

Al-Amiery, A. A., Isahak, W. N. R. W., & Al-Azzawi, W. K. (2023). Corrosion Inhibitors: Natural and Synthetic Organic Inhibitors. Lubricants, 11(4). https://doi.org/10.3390/lubricants11040174

AlGhali, B. A., Khalil, E. G., Al-Dahan, Z. T., & Jasim, I. A. (2025). USING ORTHODONTIC WIRE ELECTRODES IN GEL ELECTROPHORESIS DEVICE. Kufa Journal of Engineering, 16(2). DOI: https://doi.org/10.30572/2018/KJE/160210

Alvarez, P. E., Fiori-Bimbi, M. V., Neske, A., Brandán, S. A., & Gervasi, C. A. (2018). Rollinia occidentalis extract as green corrosion inhibitor for carbon steel in HCl solution. Journal of Industrial and Engineering Chemistry, 58, 92–99. https://doi.org/10.1016/j.jiec.2017.09.012

Asaad, M. A., Sarbini, N. N., Sulaiman, A., Ismail, M., Huseien, G. F., Majid, Z. A., & Raja, P. B. (2018). Improved corrosion resistance of mild steel against acid activation: Impact of

novel Elaeis guineensis and silver nanoparticles. Journal of Industrial and Engineering Chemistry, 63, 139–148. https://doi.org/10.1016/j.jiec.2018.02.010

Hammouti, B., Zarrok, H., Bouachrine, M., Khaled, K. F., & Al-Deyab, S. S. (2012). Corrosion inhibition of copper in nitric acid solutions using a new triazole derivative. International Journal of Electrochemical Science, 7(1), 89–105. http://electrochemsci.org/papers/vol7/7010089.

Ivosevic, S., Kovac, N., Momčilovic, N., & Vukelic, G. (2021). Analysis of corrosion depth percentage on the inner bottom plates of aging bulk carriers with an aim to optimize corrosion margin. Brodogradnja: An International Journal of Naval Architecture and Ocean Engineering for Research and Development, 72(3), 81–95. http://dx.doi.org/10.21278/brod72306

Jaddoa, H. A., Abdulhussein, B. A., & Ali, J. M. (2025). Novel efficiency of turmeric extract as a green inhibitor of low carbon steel corrosion in 3.5% NaCl solution. Case Studies in Chemical and Environmental Engineering, 11(October 2024). https://doi.org/10.1016/j.cscee.2024.101086

Kadhum, H. H., & Mohammed, M. T. (2024). EFFECT OF ZIRCONIUM ADDITION ON MICROSTRUCTURE AND PROPERTIES OF PURE TI PRODUCED BY POWDER METALLURGY. Kufa Journal of Engineering, 15(2), 106–115. DOI: https://doi.org/10.30572/2018/kje/150208

Kamburova, K., Boshkova, N., Boshkov, N., & Radeva, T. S. (2021). Composite coatings with polymeric modified ZnO nanoparticles and nanocontainers with inhibitor for corrosion protection of low carbon steel. Colloids and Surfaces A: Physicochemical and Engineering Aspects, 609, 125741. https://doi.org/10.1016/j.colsurfa.2020.125741

Mahmood, F. S., Hussein, H. Q., & Abdulwahhab, Z. T. (2022). Preparation and characterization of high surface area nanosilica from Iraqi sand via sol-gel technique. Journal of Petroleum Research and Studies, 12(4), 104–117. DOI: 10.52716/jprs.v12i4.645

Mohammed, M. (2023). CORROSION BEHAVIOR AND BIO-WETTABILITY OF THERMALLY OXIDIZED TITANIUM ALLOY SURFACE FOR BIOMEDICAL APPLICATIONS. Kufa Journal of Engineering, 14(3), 69–78. DOI:https://doi.org/10.30572/2018/KJE/140305

Saputra, R. B., Nuryoto, N., & Pramudita, M. (2025). Performance Study of Biocoating Material with Damar and Silica Extract from Rice Husk on Mild Steel in NaOH Solution.

ASEAN Journal for Science and Engineering in Materials, 4(1), 63–74. https://ejournal.bumipublikasinusantara.id/index.php/ajsem/article/view/594

Shatab, S. N., Khudair, W. S., Mohammed, M. A., & Kahthim, M. A. (2023). Corrosion in Crude Oil Distillation Units (CDUs) and a Study of Reducing Its Rates by Changing Chemical Injection Sites. Journal of Petroleum Research and Studies, 13(3), 143–161. https://doi.org/10.52716/jprs.v13i3.718 doi:10.52716/jprs.v13i3.718.

Shattab, S. N., & Alsultani, K. F. (2025). INSIGHT: PREPARATION AND CHARACTERIZATION OF SILICA FROM IRAQI SAND AS AN ECO-FRIENDLY CORROSION INHIBITOR BY USING NANOTECHNOLOGY TECHNIQUE. THE IRAQI JOURNAL FOR MECHANICAL AND MATERIALS ENGINEERING, 24(1), 175–189. DOI: https://doi.org/10.21123/bsj.2022.6895

Shnaihej, K. T., Khaleel, S. F., & Sukkar, K. A. (2019). Preparation of Nano Silica particles by laboratory from Iraqi sand and added it to concrete to improve hardness specifications. Journal of Petroleum Research and Studies, 9(3), 36–58. https://doi.org/10.52716/jprs.v9i3.313

Taheri, M., Naderi, R., Saremi, M., & Mahdavian, M. (2017). Development of an ecofriendly silane sol-gel coating with zinc acetylacetonate corrosion inhibitor for active protection of mild steel in sodium chloride solution. Journal of Sol-Gel Science and Technology, 81, 154–166. https://doi.org/10.1007/s10971-016-4180-3

Tawfik, T. A., El-Yamani, M. A., Abd El-Aleem, S., Serag Gabr, A., & Abd El-Hafez, G. M. (2019). Effect of nano-silica and nano-waste material on durability and corrosion rate of steel reinforcement embedded in high-performance concrete. Asian Journal of Civil Engineering, 20, 135–147. https://doi.org/10.1007/s42107-018-0093-5

Vorokh, A. S. (2018). Scherrer formula: estimation of error in determining small nanoparticle size. 9(3), 364–369. https://doi.org/10.17586/2220-8054-2018-9-3-364-369

Wang, X., Liu, L., Wang, P., Li, W., Zhang, J., & Yan, Y. (2014). How the inhibition performance is affected by inhibitor concentration: a perspective from microscopic adsorption behavior. Industrial & Engineering Chemistry Research, 53(43), 16785–16792. https://doi.org/10.1021/ie502790c

Yousif, I., & Ataiwi, A. (2018). Construction of slurry jet erosion tester and the effect of particle size on slurry erosion. Kufa Journal of Engineering, 9(3), 17–25. https://doi.org/10.1021/ie502790c.